Chapter 3
Observations of the Perseid Meteor Shower[1]

3.1 Introduction

The Perseid meteor shower, which recurs annually near August 12, is among the most studied meteor showers of the present era. Hasegawa (1993) has noted that based on ancient records of its activity, the Perseids are among the oldest of all recorded showers,

During the Perseid returns of the 1860's, the first crude orbit determination of the stream was made by Schiaparelli (1867) who noted the stream's orbital similarity to the recently discovered comet 109P/Swift-Tuttle (1862 III), which has a period of just over 130 years. This was the first direct evidence connecting comets and meteor showers. Kronk (1988) has given a detailed historical review of the shower.

Many groups for the remainder of the 19th century and well into the 20th century carried out visual observations of the shower. These data provide our only direct measure of the activity from the shower until the middle of the 20th century and the advent of radar. These early observations were very inconsistent, as the methods used by individuals and sometimes groups of observers differed radically and were employed under widely varying sky conditions. As a result, determining the level of Perseid activity during most of the 19th and 20th century is problematic.

Interest in the Perseids increased during the late 1970's in anticipation of the return of 109P/Swift-Tuttle, which was expected to reach perihelion circa 1980 (Marsden, 1973). Meteor observations carried out during the late 1970's suggested activity was increasing toward a peak in the early 1980s, heralding 109P/Swift-Tuttle's return (Kronk, 1988). The comet, however, was not recovered within this time period.

---

[1] A version of this chapter has been published : P. Brown and J. Rendtel (1996) The Perseid Meteoroid Stream: Characterization of Recent Activity from Visual Observations, *Icarus*, **124**, 414-428.

In 1988 and more notably in 1989, a new “peak” was identified approximately 12 hours before the long-recognized “normal” stream maximum (located at 140.1° (J2000.0)) which was of similar strength to the regular maximum (Roggemans, 1989; Koschack and Roggemans, 1991). This new peak was widely interpreted as representing the early detection of newer meteoroids associated with the impending return of 109P/Swift-Tuttle. The position of the new peak in these years was very close to the nodal longitude of the comet (Ω=139.44°), which was ultimately recovered in September 1992 (Yau et al., 1994). Beginning in 1991, the Perseids have displayed strong outbursts in activity associated with the return of the parent comet 109P/Swift-Tuttle, which has continued through, to the late 1990’s.

The best set of data recording these outbursts has been visual observations of the Perseids made by amateur astronomers. The quantity and uniformity of the observations permit precise reconstruction of the activity and flux profile of the stream at an unprecedented level. In what follows, we analyse the detailed visual activity of the Perseid meteor shower near its time of maximum for the years 1988-1994. In total, the visual meteor data consist of some 14,552 counting intervals, collected by 1,115 meteor observers from 38 countries who reported 243,227 Perseid meteors during 14,237 hours of effective observational time over these seven years. From these data we have selected subsets which met all our criteria for inclusion in this work (see Sect. 6.2) and summarized the final dataset in Table 3.1. The activity of the shower is characterized by both the Zenithal Hourly Rate (ZHR) and flux, Φ, along with their associated errors. Particle characteristics within the stream are represented through the population index (r) of the shower at specific points along the Earth's orbit. These are the basic quantities defining the stream, which could be derived from these observations.

3.2 Collection of Observations and Methods of data Reduction.

The methods used to observe meteors and reduce these data follows from the development of the visual techniques summarized by Kresakova (1966). Here we give an abbreviated qualitative discussion; for more detailed discussions; readers should refer to Koschack and Hawkes (1995) and Koschack (1995). Of importance is the fact that these techniques are applicable to single observers only; group observations, where data are pooled, cannot be used in this method.

In the most basic form, an individual observer uses only the naked eye to count the number of meteors seen during a specified time interval and then either associates each with a certain shower or records it as a sporadic meteor while noting the magnitude of each meteor. During this time, the observer also notes the faintest star visible in his/her field of view (denoted the limiting magnitude (LM)) and records the total effective time that the sky was actually monitored (T_{eff}). The LM is typically the result of a weighted mean of several such measurements taken during the observation at intervals determined by changing sky conditions and reported as averages to 0.01 M_v.

From each observation interval a quantity called the Zenithal Hourly Rate (ZHR) is calculated. The ZHR is the number of meteors from the shower a standard observer would see under unobstructed skies with the radiant point overhead and the LM=6.5. This definition forms the basis for “standardization”; the goal of all reductions is to correct an imperfect observation to this standard. To characterize the particle population, we define the population index *(r)* as:

$$r = \frac{N(M_v + 1)}{N(M_v)} \tag{3.1}$$

where $N(M_v)$ is the cumulative number of meteors of magnitude M_v or brighter. The population index characterizes the slope of the cumulative number of meteors vs their magnitude for the shower and can be related to the differential mass index *s* with appropriate connection between mass and magnitude via (McKinley, 1961):

$$s = 1 + 2.5\log(r) \tag{3.2}$$

Using the population index along with the ZHR we are able to compute the flux in units of meteoroids km^{-2} $hour^{-1}$. Further details relating to the derivation of these quantities can be found in Koschack and Rendtel, 1988; Koschack and Rendtel, 1990a,b; Koschack, 1995 and Brown and Rendtel 1996.

3.3 Results of Perseid Observations 1988 - 1994

The ZHR activity, population index and corresponding flux profiles for the Perseid stream for each year from 1988-1994 are given in Figs. 3.1-3.7. Not shown in these figures are the sporadic hourly rates (HR) corrected for stellar limiting magnitude. These values are used during the initial selection cycle as indicators to aid in the detection of systematic errors in the shower ZHRs. Since observers contributing to the ZHR average at a given time are distributed over areas of order the size of a continent, the sporadic HR is not correctable in the same manner as the shower HR, a direct result of the fact that sporadic meteors do not have radiants which are uniformly over the celestial sphere (cf. Jones and Brown, 1993), but rather are concentrated in several diffuse sources. This implies that the sporadic HR varies as a function of geographic latitude and local time in a non-trivial manner and thus cannot be used accurately to correct relative shower rates from different locations.

Inspection of these curves shows that the level of flux appears to vary significantly throughout these years not only in the outburst component of the profile, but in the primary maximum as well. Some of this variation is due to lunar conditions as in 1990 and 1992. As a result, the corresponding profiles are uncertain, the effect being most evident in the large errors in the population index profiles in these years, caused by low limiting magnitudes and thus small numbers of faint meteors. The number of Perseid meteors, the total effective observing time and the number of contributing observers for each year are given in Table 3.1. The profiles also differ in some cases due to poor observer coverage, particularly in the Pacific region, and result in gaps during several years.

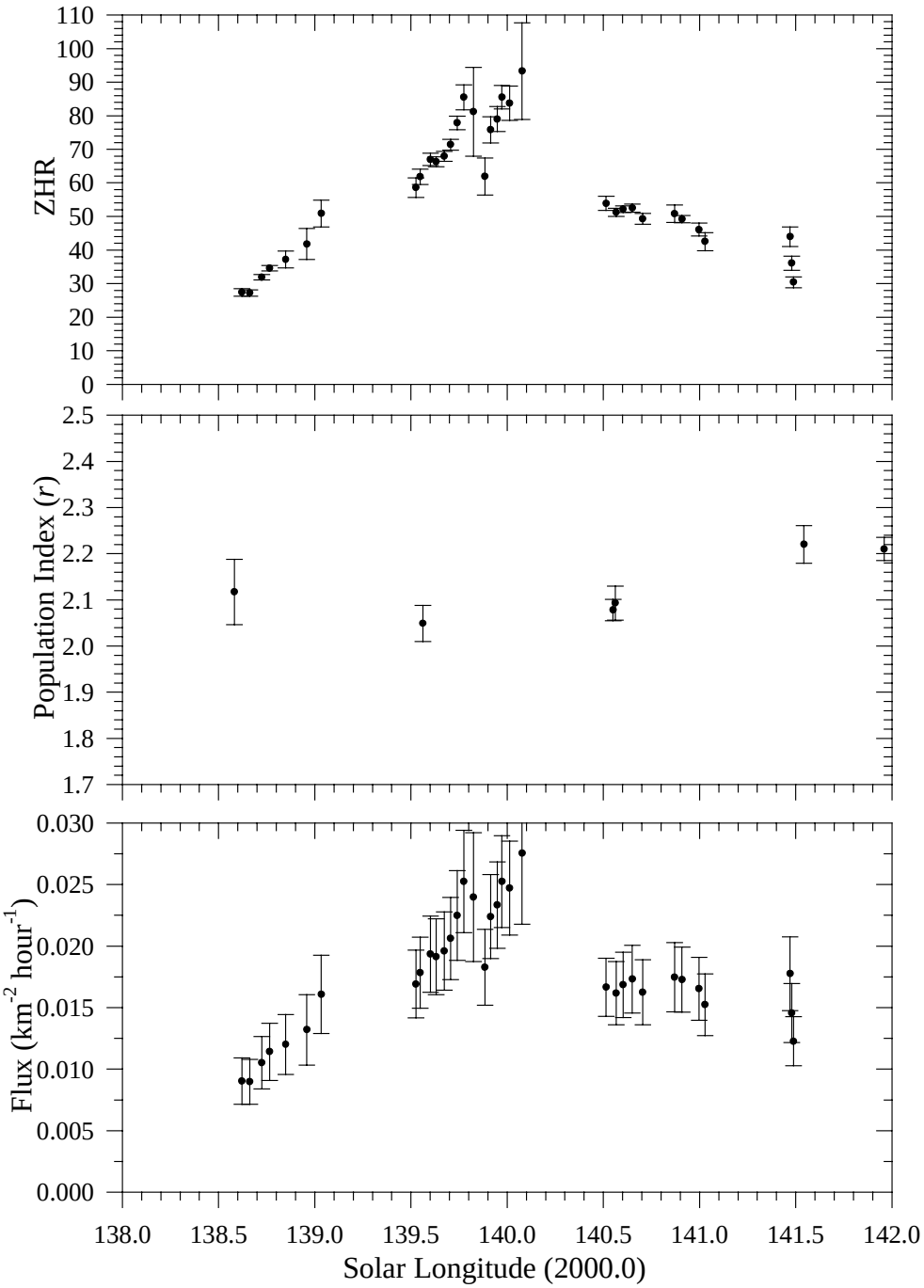

Figure 3.1: The ZHR (top), population index (middle) and flux (bottom) for the 1988 Perseid return.

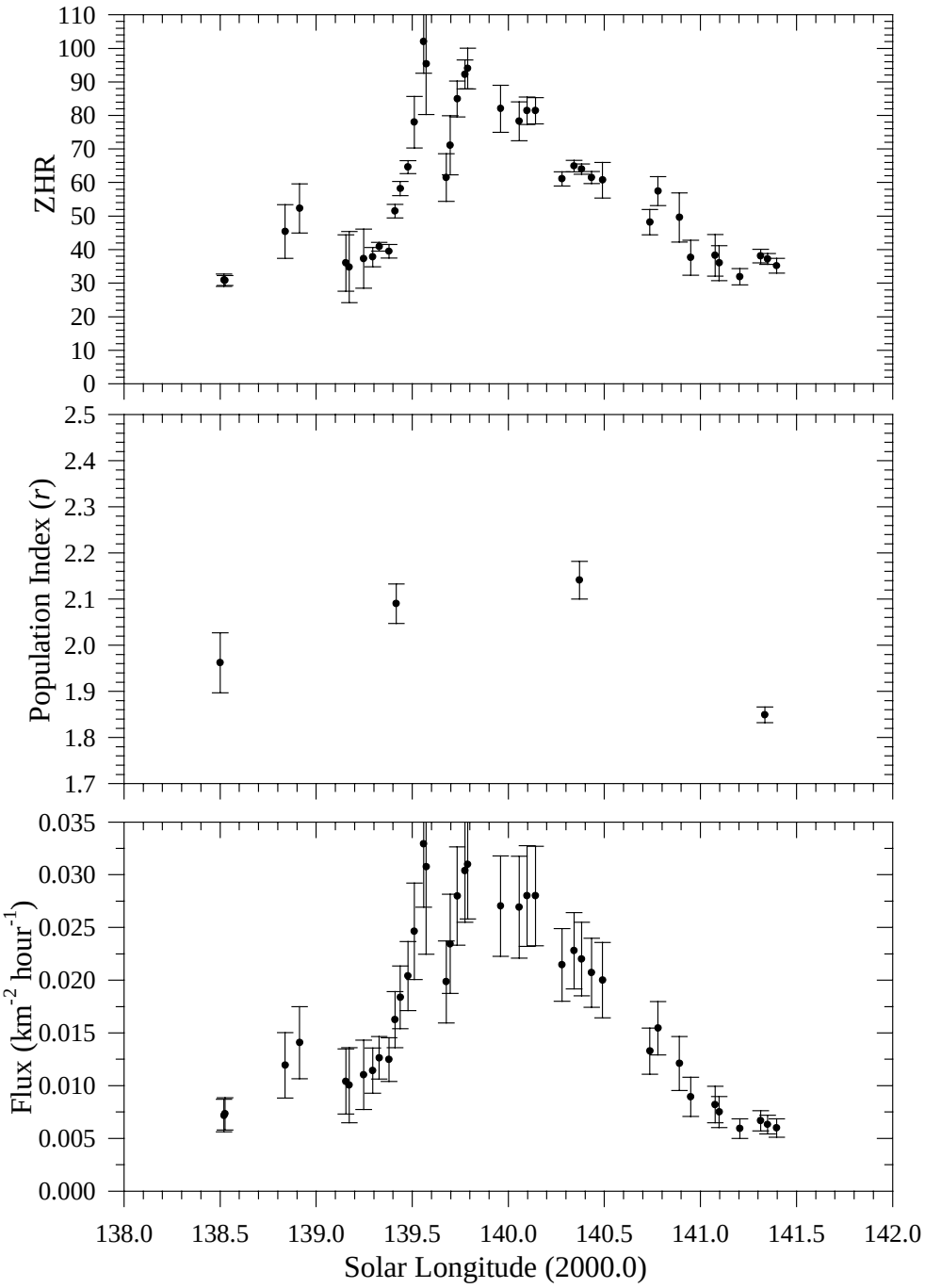

Figure 3.2: The ZHR (top), population index (middle) and flux (bottom) for the 1989 Perseid return.

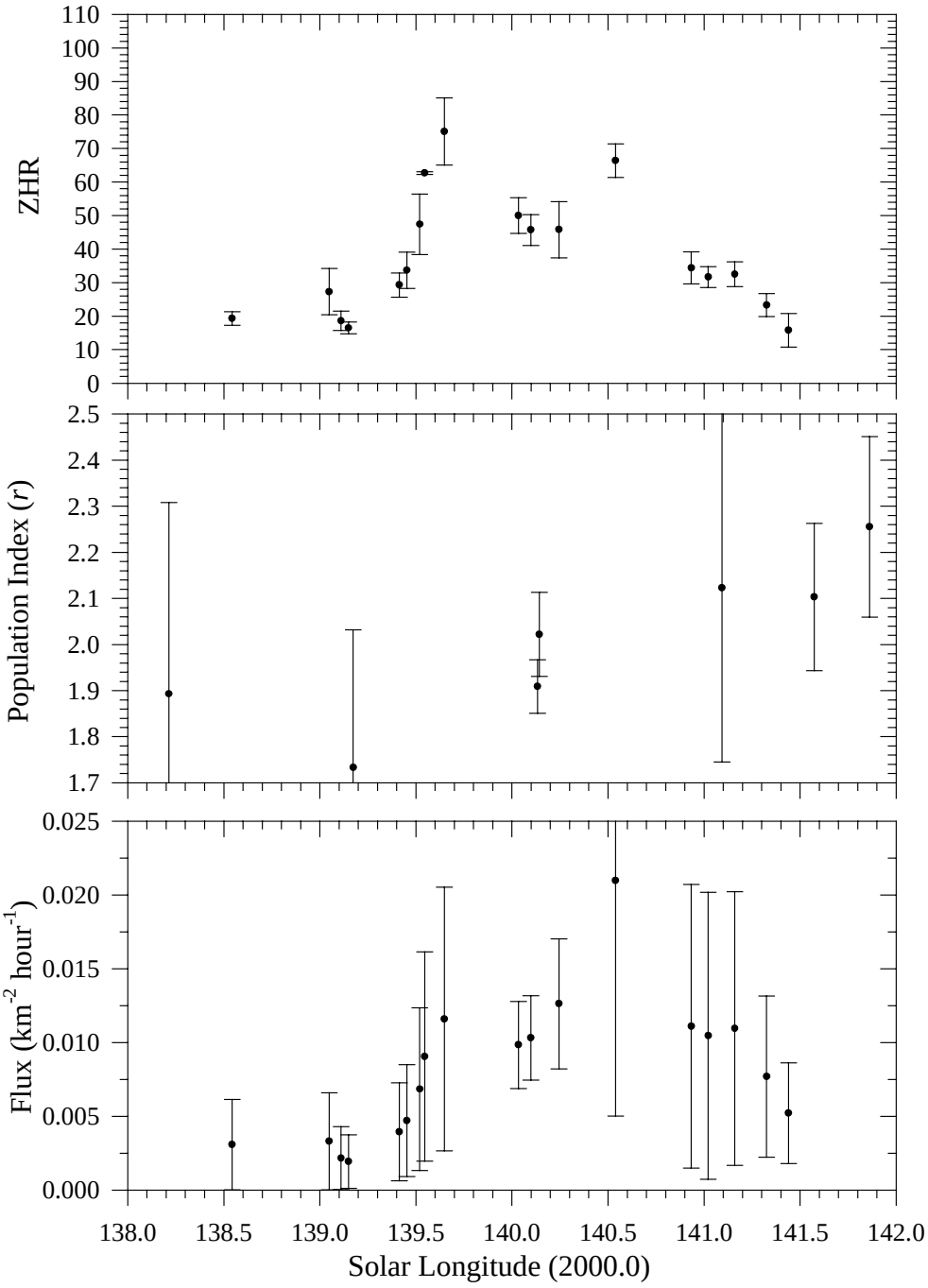

Figure 3.3: The ZHR (top), population index (middle) and flux (bottom) for the 1990 Perseid return.

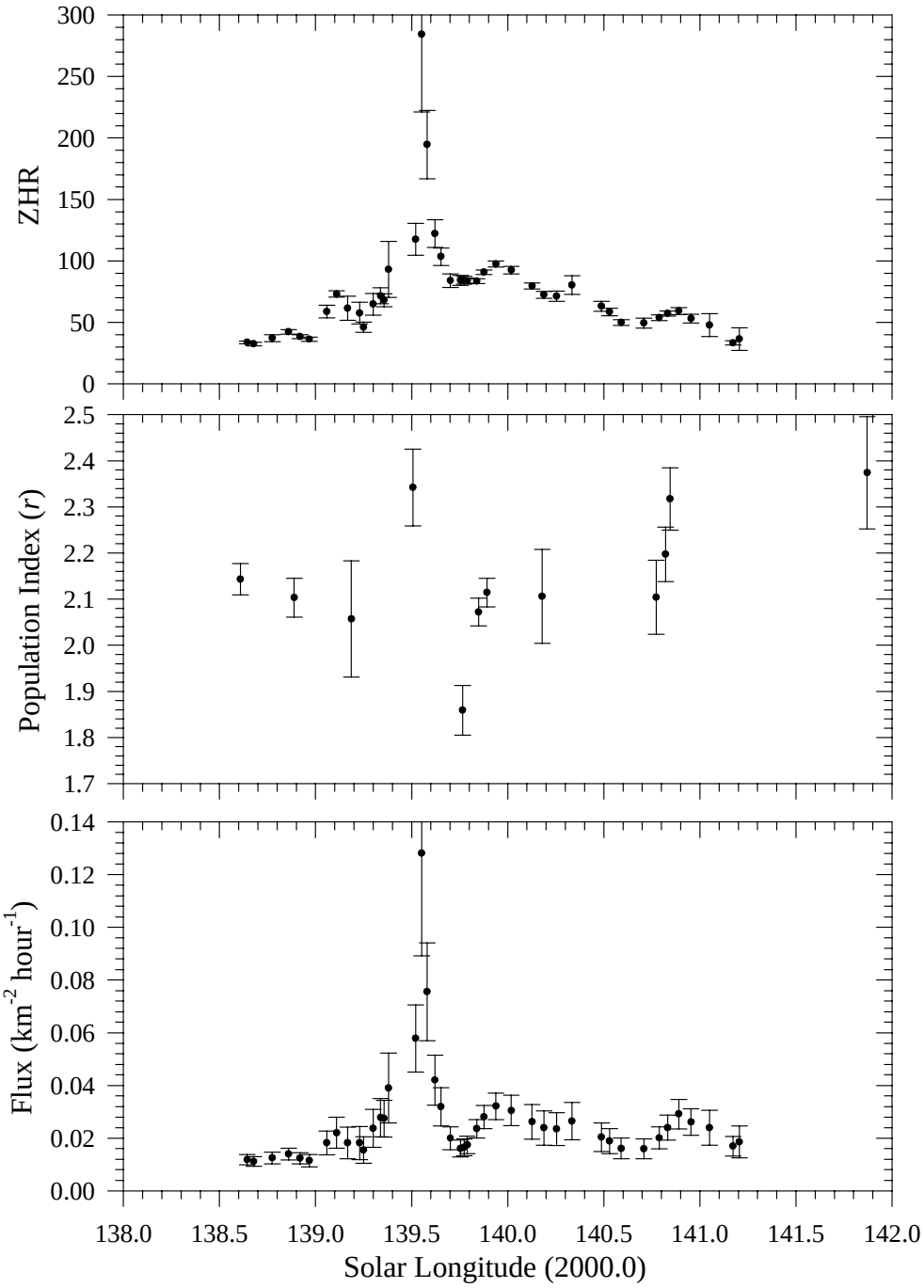

Figure 3.4: The ZHR (top), population index (middle) and flux (bottom) for the 1991 Perseid return.

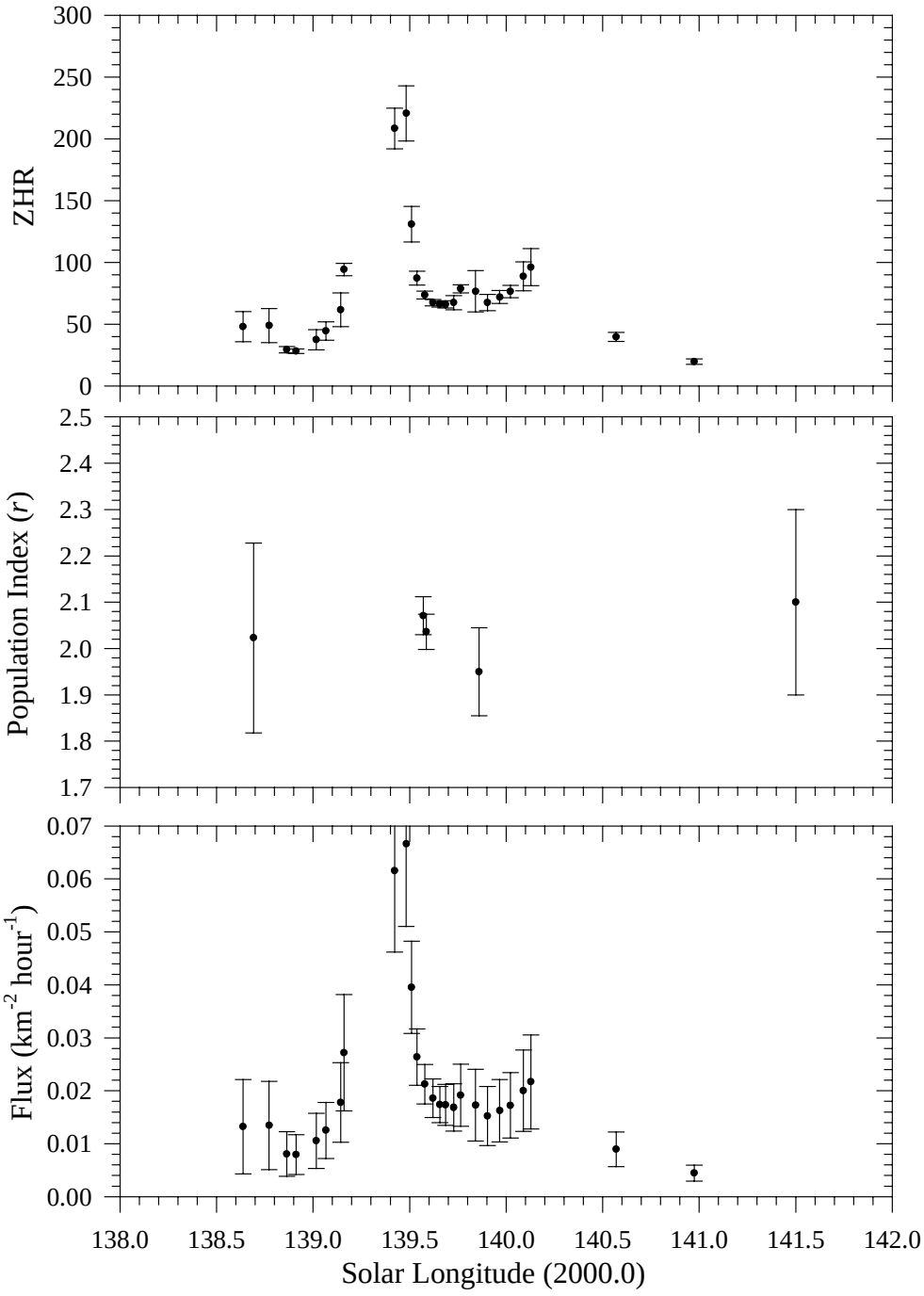

Figure 3.5: The ZHR (top), population index (middle) and flux (bottom) for the 1992 Perseid return.

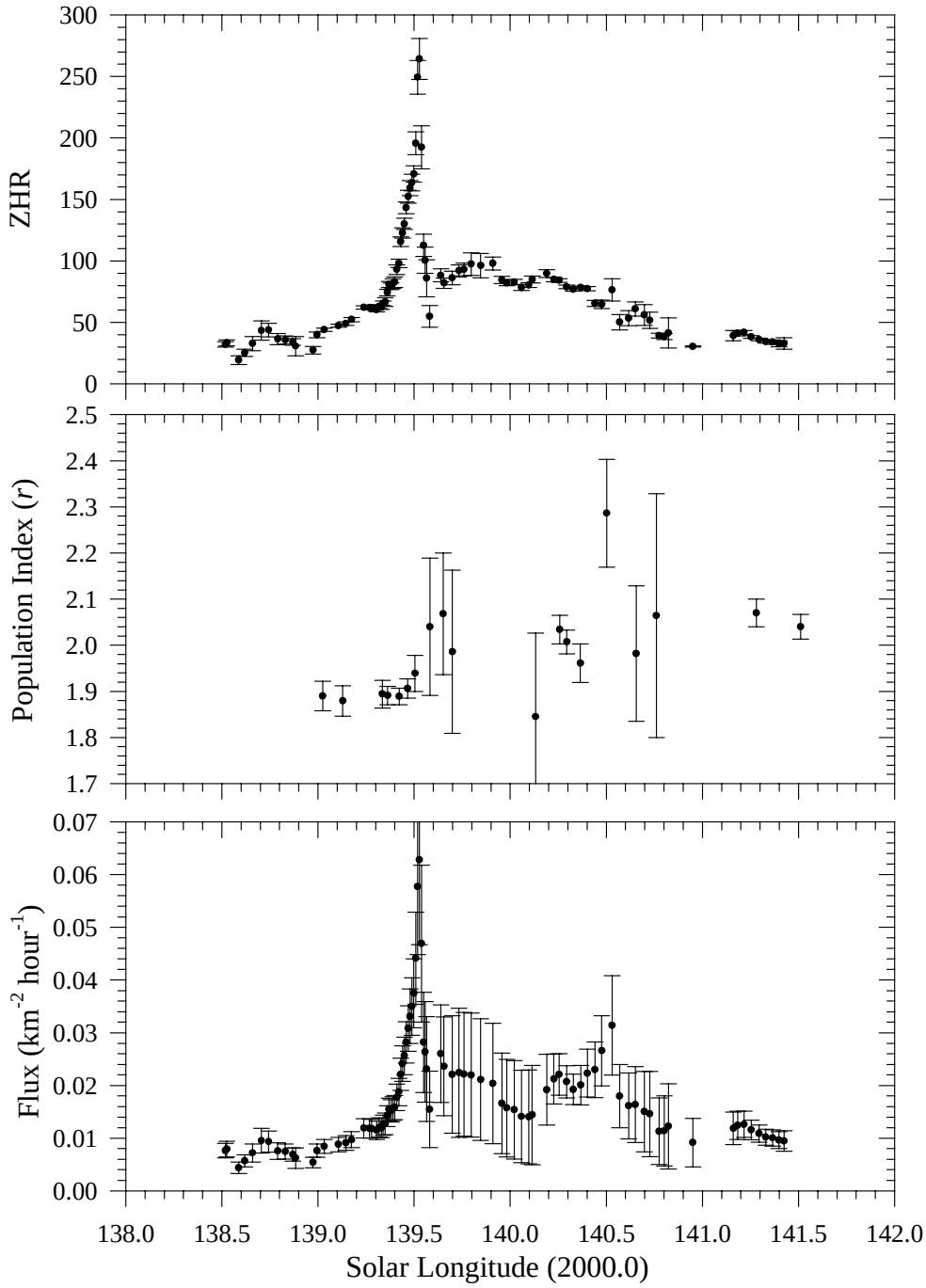

Figure 3.6: The ZHR (top), population index (middle) and flux (bottom) for the 1993 Perseid return.

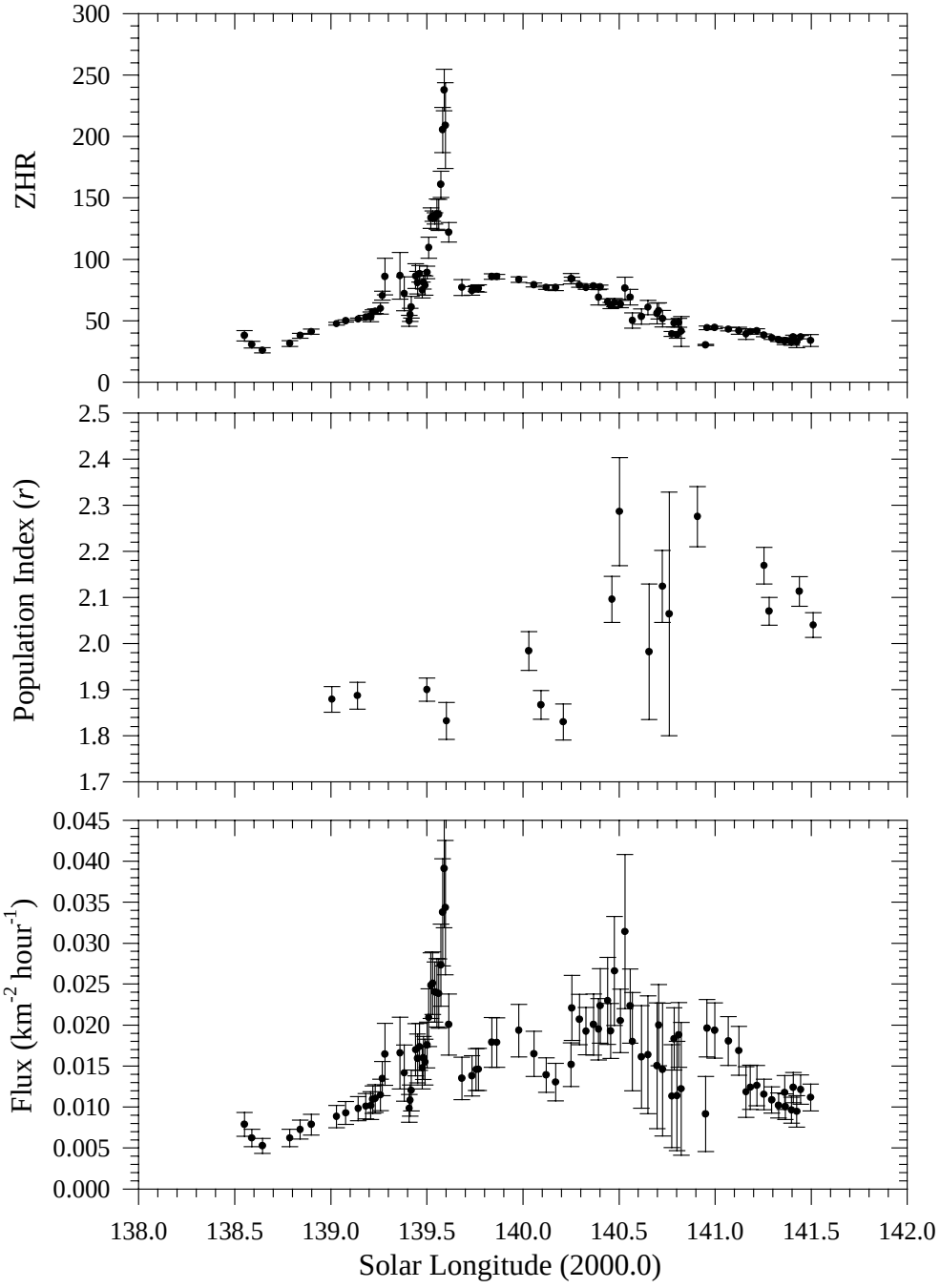

Figure 3.7: The ZHR (top), population index (middle) and flux (bottom) for the 1994 Perseid return.

Despite these difficulties, the large datasets clearly show that the level of Perseid activity varies from year to year. The shapes of the ZHR and flux profiles are generally similar, though significant variations in the population index, particularly after the main maximum, do tend to broaden the main peak of the latter. The flux curves shown here are for a limiting absolute magnitude of 6.5, or an equivalent limiting mass of 2×10^{-8} kg using the mass-magnitude-velocity correction of Verniani (1973). For the outburst portions of the profile, fainter meteors will tend to be under-represented as observers become overloaded recording shower meteors. This saturation effect has been documented in previous examinations of Perseid data (Koschack et al. 1993). The effect will be to make the flux values smaller than the true values; hence the values shown here for the new peaks are lower limits.

In 1988, the data are well distributed about both maxima. This was the first year that the "new" maximum was detected, in this case at λ=139.78°about 6 hours before the traditional peak which took place at 140.08° (Roggemans, 1989). The old and new

Table 3.1: The number of Perseid Meteors, the total effective observing time and the number of contributing observers for each year of the study. The numbers in parentheses represent the values for the average Perseid reference profile. The latter are not simple sums of the previous rows due to the exclusion of the time periods containing the outburst peak in the reference profile.

Year	Number of Perseids	Total Observing Time (hours)	Number of Observers
1988	22,526 (38,037)	1033 (2571)	194 (230)
1989	16,708 (25,227)	647 (1930)	187 (261)
1990	1,547 (3,877)	115 (863)	46 (137)
1991	36,073 (44,762)	1045 (2079)	219 (262)
1992	6,462 (10,870)	326 (1290)	105 (195)
1993	59,080 (81,538)	1768 (3211)	409 (454)
1994	33,210 (47,165)	1041 (2428)	268 (347)
1988-1994	206,872 (251,476)	13,538 (14,372)	1089

maxima were of very similar activity, but there are insufficient magnitude data to determine whether or not the particle composition differed between the peaks. The ascending branch of the early maximum is well defined and shows a half-width-to-half-maximum (HWHM) activity above the general profile of one hour. The descending branch is not well defined, but the few data here suggest a similar decline to a local minimum before activity again increases to the normal maximum. The descending branch of the main maximum is missing in these data and a higher maximum than shown here is possible, though the data do cover the interval during which the normal Perseid peak traditionally occurs and also where it is well defined in later data. The population index profile suggests a local dip of order a day in scale in the *r* value near the time of peak relative to the days before and after the maxima.

The 1989 profile in Fig 3.2 is similar to 1988 for times away from the maxima. The early maximum occurs at 139.56° while the normal maximum is at 139.8°. The magnitudes of the maxima are again very similar. The ascending branch of the early peak has a HWHM of two hours and is well defined. The descending branch from the early peak is absent in 1989 due to uneven observer coverage. The rising portion of the main profile shows a clear peak followed by several closely spaced points of decline, suggesting the maximum is better located than in 1988. Several features are notable in the falling portion of the main maxima, namely at 140.1° and 140.3°.

Data for 1990 are heavily contaminated by the moon, which was full on 6 August 1990 and thus affected all observations during the peak interval. Few observations made under good conditions were available. There appears to be a first peak near λ=139.6° with a maximum value of roughly 75, with the later peak occurring near λ=140.5° and having a ZHR value of 66. The extremely low ZHR values at peak are likely artifacts of the lunar conditions. Additional error is apparent from the shape of the sporadic activity curve, which closely mimics the Perseid curve, suggestive of numerous Perseids being counted as sporadic.

In 1991, the relative magnitudes of the two peaks become quite different, with the early peak dominating. The peak times for the maxima are clearly resolved as

λ=139.55° and λ=139.94° respectively. The ascending branch of the early peak has few data, but the HWHM can be roughly estimated as 0.5 hours. The descending portions have good coverage and reveal a HWHM of only one hour. The normal peak shows good coverage in 1991, displaying a HWHM value of 12 hours for the descending branch, but the ascending branch value is uncertain due to contamination from the earlier peak. Additional activity features after the main maximum are prominent in this profile, occurring at λ=140.34° and 140.9°. There is also an apparent difference in particle makeup across the broader profile, with a local minimum for *r* between the early and main maximum.

The lunar conditions near the shower peak were poor in 1992, with the full moon occurring on August 13. Nevertheless, good data coverage enables better determination of the time of the peak and its magnitude than in 1990. Information is obtainable about the descending portion of the early peak which was approximately one hour HWHM and occurred at λ=139.48°, while the main maximum appears at approximately λ=140.13° with a magnitude of 90.

The 1993 shower had the best coverage of all years in this study. The profile in the ascending branch of the early peak is the clearest of any of the profiles, displaying a HWHM of 1.5 hours. The descending branch is not well defined, but these data do suggest that the HWHM for the ascending branch was almost twice as wide as for the descending branch, with the early peak occurring at λ=139.53°. The main ZHR maximum was broad in extent, but occurred near λ=139.9°. A prominent secondary peak in both the ZHR and flux profiles after the main maximum is located at λ=140.2°; the flux profile also suggests that a secondary maximum in flux occurred at λ=140.5° accompanying a large increase in *r*.

In 1994 good observer coverage and excellent lunar conditions converged. The ascending portion of the profile is again well established with the early maximum having occurred at λ=139.59° and displaying a HWHM of only one hour. The magnitude data are particularly well defined in 1994 and show a decrease in *r* after the early peak. A strong asymmetry is present in the population index before and during maximum as compared

to after both peaks when its value gets much larger. The main peak occurs at λ=139.9°.

These results are summarized below in Table 3.2.

Table 3.2: The locations and magnitudes of the Perseid maxima from 1988 to 1994. λ_1 is the position of the new (outburst) maximum and λ_2 is the position of the main or normal maximum. The peak fluxes associated with the first peak ($\Phi_{6.5\ outburst}$) and with the normal maximum ($\Phi_{6.5\ peak}$) are given in units of $\times 10^{-2}$ meteoroids km^{-2} hr^{-1} for Perseid meteors brighter than absolute magnitude +6.5.

Year	λ_1	$ZHR_{outburst}$	$\Phi_{6.5\ outburst}$	λ_2	ZHR_{peak}	$\Phi_{6.5\ peak}$
1988	139.78±0.03°	86±4	2.5±0.4	140.08±0.04°	106±22	2.4±0.4
1989	139.56±0.03°	102±10	2.6±0.3	139.80±0.09°	94±6	3.1±0.5
1990	139.55±0.05°	75±10	1.1±0.9	140.54±0.2°	81±61	1.7±0.1
1991	139.55±0.03°	284±63	13±4	139.94±0.04°	97±2	3.2±0.5
1992	139.48±0.02°	220±22	6.7±1.6	140.13±0.2°	84±34	2.5±0.4
1993	139.53±0.01°	264±17	6.3±1.6	139.91±0.04°	86±2	2.0±1.1
1994	139.59±0.01°	238±17	3.9±0.7	139.84±0.04°	86±2	1.8±0.3
1988-94	-	-	-	139.96±0.05°	86±1	2.5±0.4

3.4 High Temporal Resolution Profiles

To determine if any structure is present in the outburst component of the stream, the data for 1993 and 1994 near the locations of the outburst have been re-analyzed at higher temporal resolutions. Small-scale variations in flux-profiles near the time of outbursts have been reported in the past with the Draconids (Lovell 1954, p.330) and α-Monocerotids (Rendtel et al., 1996). Here all individual counting intervals greater than 0.5 hours were rejected to obtain a high resolution profile with steps as short as 0.004° in the solar longitude in the immediate region near the outburst peak. Strictly speaking, these averaging intervals would be too short if they consisted predominately of 0.5 hour (or longer) counting intervals, but fortunately most count intervals in this period are of the order of 5-15 min duration. The results are shown in Figs 3.8 and 3.9 where details of the averaging intervals and step lengths are given. Note that the 1993 data are more than an order of magnitude more plentiful than the 1994.

The buildup to the maximum in 1993 is extremely well-defined and shows two main components. The first is a gradually increasing branch which begins at λ=139.35° and continues to λ=139.49°. In this interval, the slope of the flux - solar longitude curve is 2×10^{-3} meteoroids km^{-2} hour^{-1} per 0.01° of solar longitude brighter than +6.5 (hereafter (M_v >6.5) 0.01°$^{-1}$). The second component is the interval from 139.49° - 139.53° where the slope changes dramatically to ~10^{-2} (M_v >6.5) 0.01°$^{-1}$. These two sections suggest that the outburst may itself consist of several sub-components of differing ages with the steep increase being associated with the most recent ejecta and the broader increase just before it being due to material diffused somewhat from slightly older passages of Swift-Tuttle. Since the nodal longitude of Swift-Tuttle has been gradually increasing over time, one expects the oldest ejecta to be before the current nodal longitude of the comet.

This effect is further reflected in the descending component of the profile. Though less defined, it shows a steep decrease, having a mean slope of -2.6×10^{-2} (M_v >6.5) 0.01°$^{-}$

[1] in the interval 139.53°-139.55°. The profiles in both the ascending and descending portions of the outburst in 1993 are relatively smooth. Only hints of slight variations near 139.45° and 139.39° are present. Similar structures are also visible in the 1994 profiles near 139.43° and 139.51°. Of interest is that the first of these is in a location similar to the structure present in 1993 and both are extremely close to the current nodal longitude of 109P/Swift-Tuttle. The latter fluctuation in 1994 corresponds closely to the location of maximum in 1993 and suggests that many of the meteoroids associated with the outburst maxima have a small spread in their semi-major axis, amounting to only a few tenths of an A.U. or are perturbed into Earth-intersecting orbits effectively for intervals of order a year.

In 1994, the buildup to the outburst peak is much slower than in 1993, first showing a plateau and then a jump in activity near 139.51°. The slope of the steeper ascending section of the outburst from 139.57° - 139.59° is 1.3×10^{-2} (M_v >6.5) $0.01^{\circ-1}$, very similar to the slope found in 1993. The descending branch of the profile has a slope of -1.4×10^{-2} (M_v >6.5) $0.01^{\circ-1}$ from 139.59° - 139.61° which is significantly less than in 1993, though the descending portions of both profiles are not well covered.

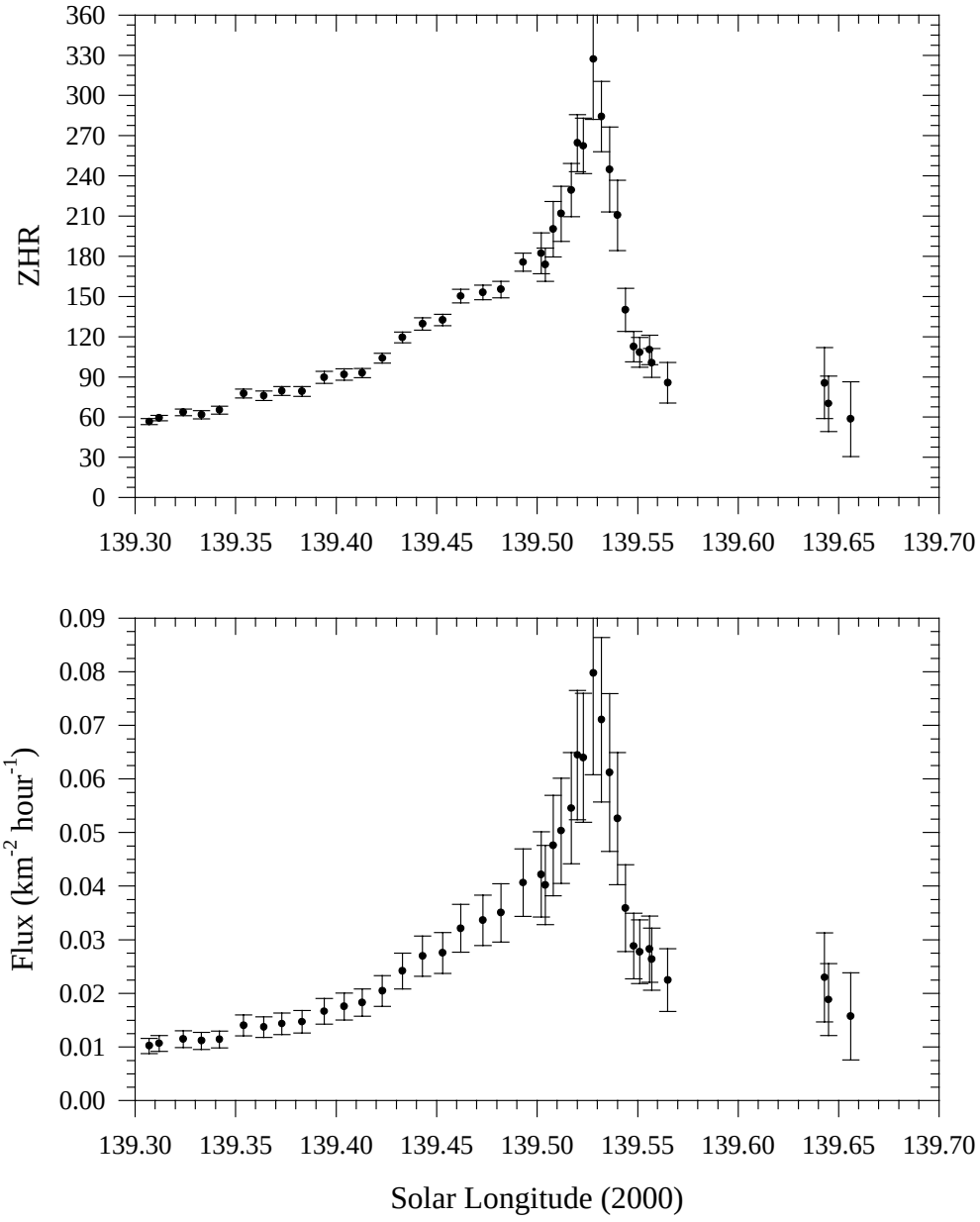

Figure 3.8: The ZHR (top) and flux (bottom) for the 1993 Perseid return. A total of 1260 count intervals, shorter than 0.3 hours in the central interval and less than 0.6 hours in the outer intervals, were used. Between λ=139.3° to 139.5° and 139.56° to 139.7°, the sampling interval was 0.02° shifted by 0.01°, while from 139.5°-139.56° the sampling window was reduced to 0.008° shifted by 0.004°.

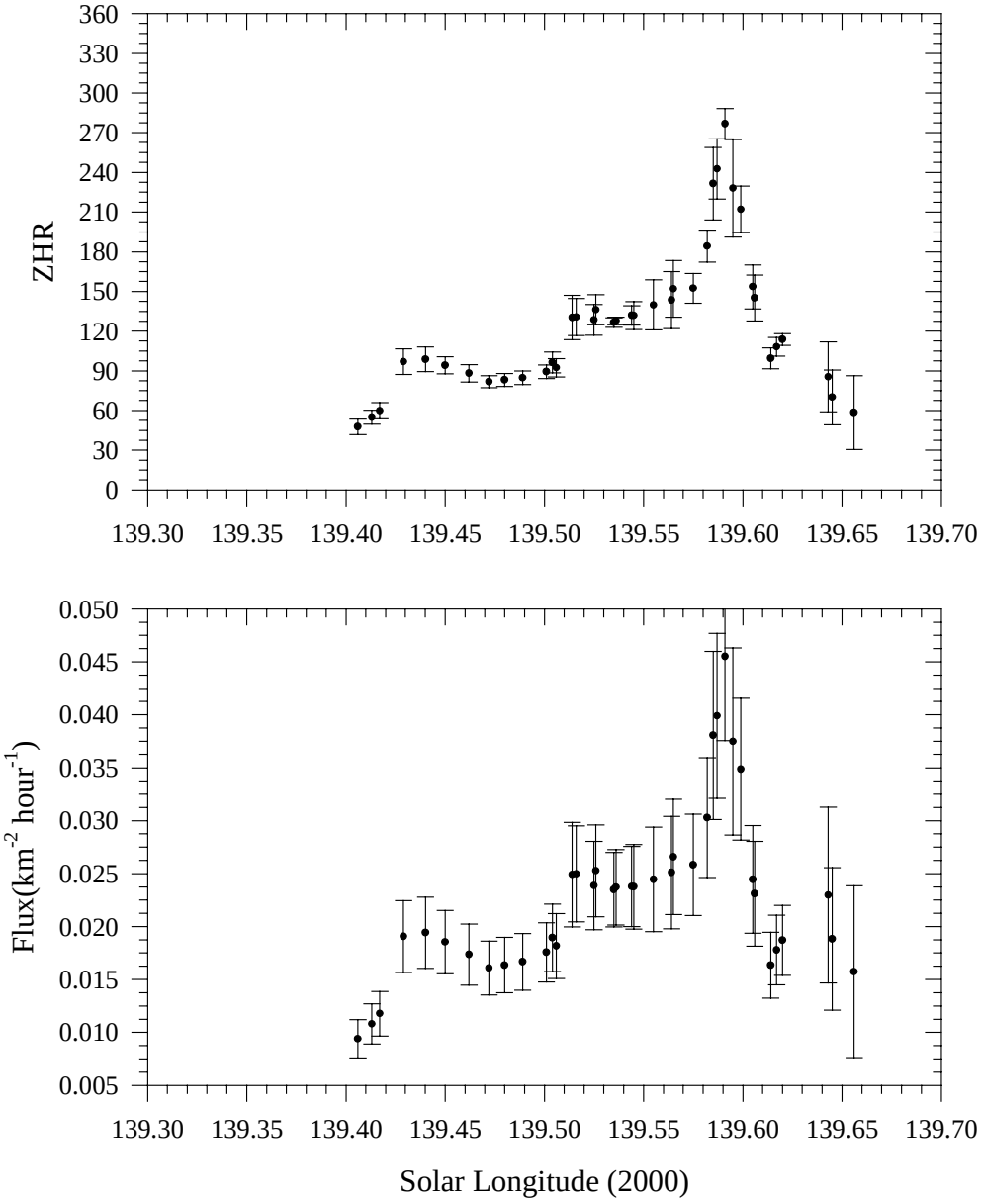

Figure 3.9: The ZHR (top) and flux (bottom) for the 1994 Perseid return. A total of 124 count intervals shorter than 0.3 hours in the central interval and less than 0.6 hours in the outer intervals were used. Between λ=139.3° and 139.5° and 139.62°-139.7° the sampling interval was 0.02° shifted by 0.01° while from 139.5°-139.62° the sampling window was reduced to 0.008° shifted by 0.004°.

3.5 Discussion

The Perseid stream, as described from the visual observations presented here, can be delineated broadly into three major components: a broad plateau displaying weak activity (background Perseids); a more concentrated component centred about the traditional Perseid peak (core Perseids); and a strongly time-varying component of short duration which appears in all profiles shortly after the nodal longitude of the parent comet (outburst Perseids). To see more clearly the first two components, which have only modest variations from year to year, we have synthesized a mean Perseid curve from all available visual observations from 1988-1994, but excluded those intervals showing the outburst component. The ZHR profile for this average curve, the associated sporadic rate, the mean population index profile and the flux profile are given in Fig 3.10 for the full period of Perseid activity. These same quantities are also shown for the ten day interval centred about the main Perseid peak in Fig. 3.11.

The background component is long-lived and shows weak activity extending from late July (~115°) until the end of August (~150°). This portion of the Perseid stream shows a very gradual increase in activity until ~ 138°, at which time the activity profile steepens as the core portion of the stream is encountered. The core component rises to a peak whose average position is λ=139.96°±0.05°. The steepest section of the peak associated with the core Perseids is very symmetrical, the ascending portion having a HWHM of 1.06°±0.07° compared to the descending profile with a HWHM of 1.04°±0.07°. A slight asymmetry in the overall shape of the ZHR curve is most evident at the 1/4-width points, located 2.58°±0.07° before maximum and 2.35°±0.07° after maximum. From these results, the Perseid shower is above the sporadic background from ~ 136°-143° or roughly one week.

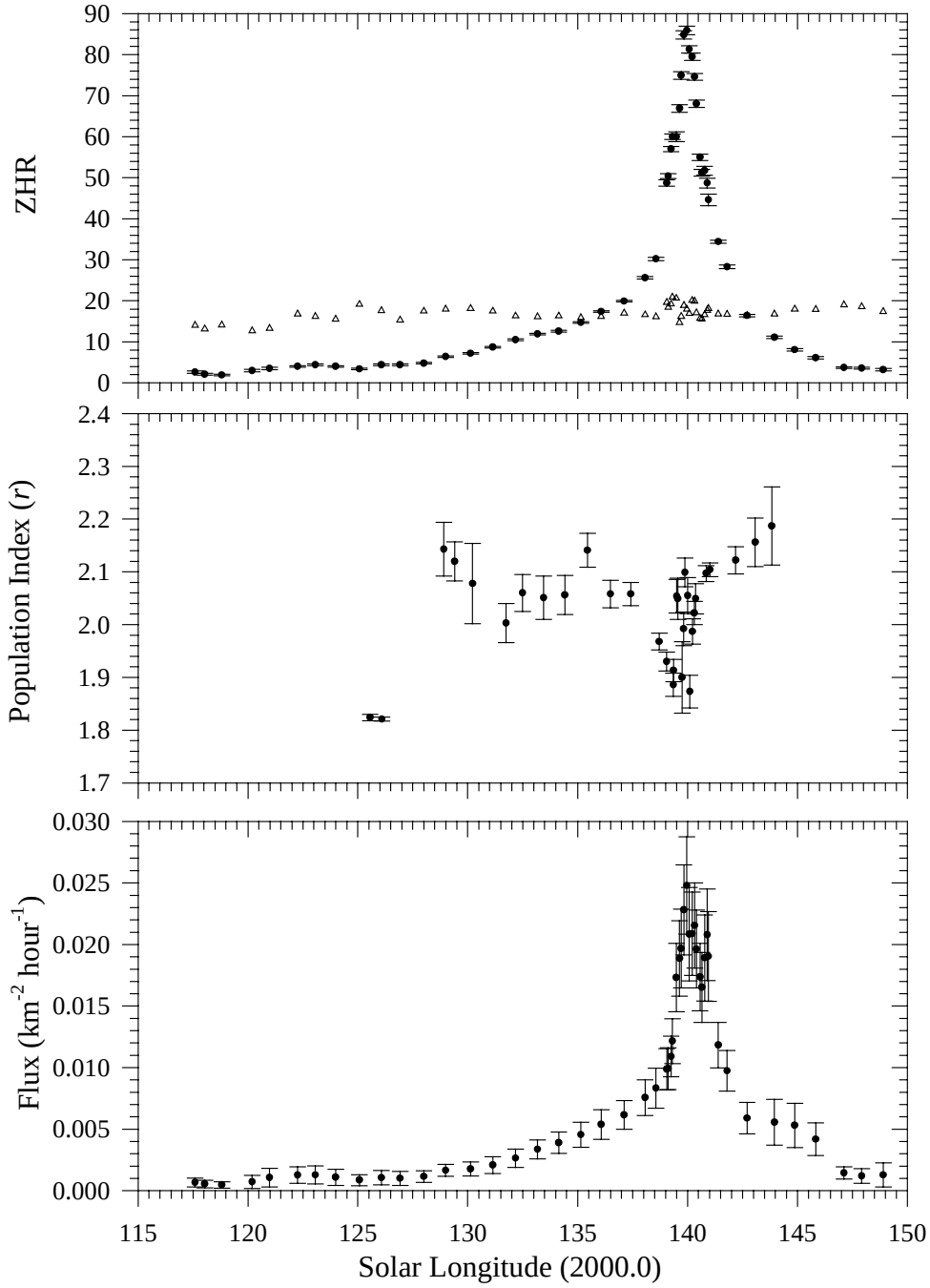

Figure 3.10: The ZHR (top), population index (middle) and flux (bottom) for the mean Perseid activity profile (1988-1994) along with the associated sporadic hourly rates denoted by Δ for the full period when visual Perseid activity is detectable visually.

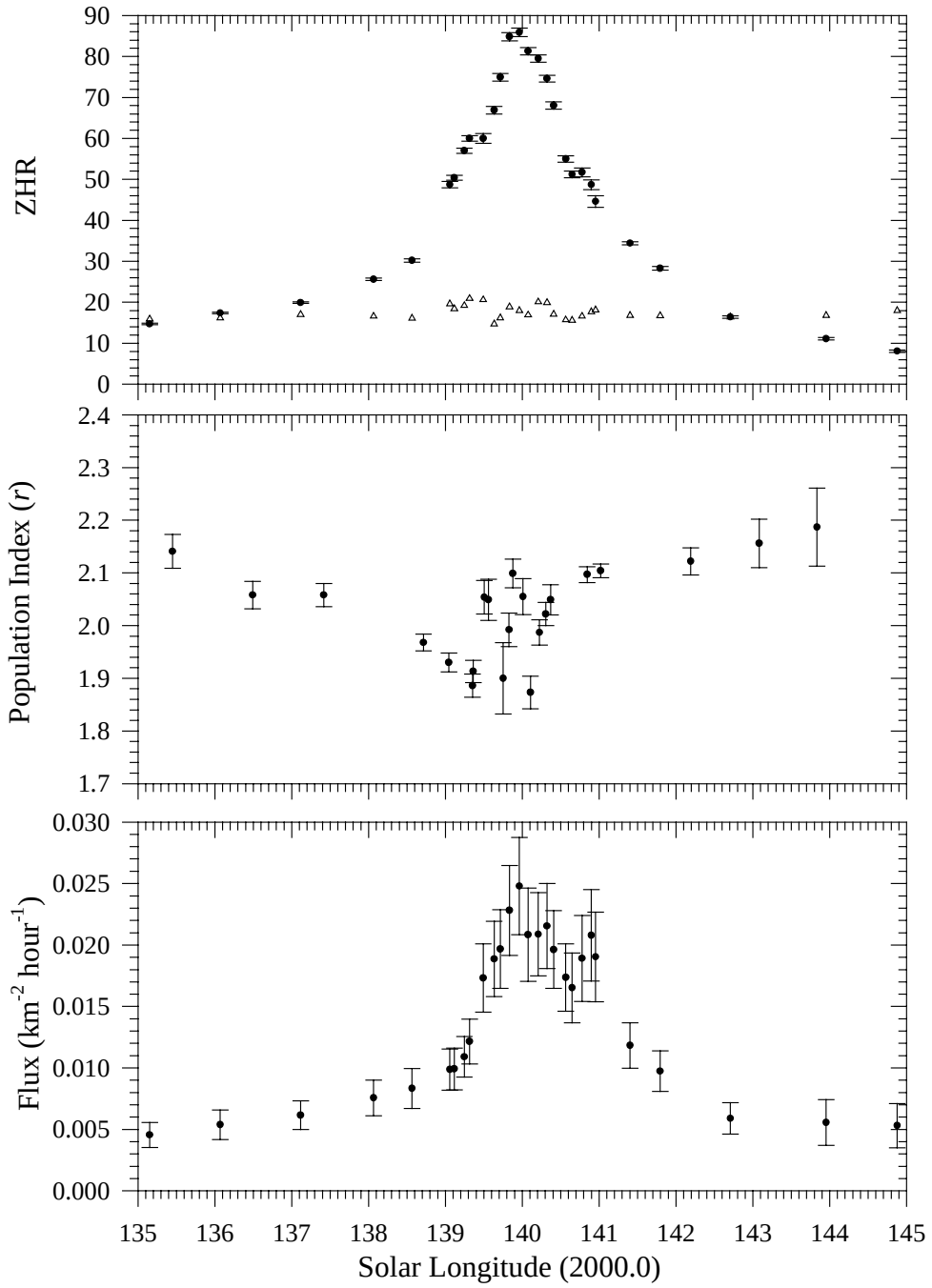

Figure 3.11: The ZHR (top), population index (middle) and flux (bottom) for the mean Perseid activity profile (1988-1994) along with the associated sporadic hourly rates denoted by Δ for the 10-day interval centred about the main Perseid peak.

That the average Perseid profile is a superposition of two components and is asymmetrical has been known for some time from visual observations (cf. Ahnert-Rohlfs 1952, Lindblad 1986, Mason and Sharp 1981, Zvolankova 1984) as well as radar data (Simek and McIntosh 1986, Lindblad and Simek 1986, Simek 1987). Harris et al. (1995) have modelled the overall activity of the stream through decay of 109P/Swift-Tuttle over a 160,000 year time period. Their model reproduces the asymmetry in the core portion of the stream and also predicts several strong secondary maxima before the main peak, most notably one lasting several days at λ=125°. Such secondary maxima are not present in the mean profile presented here. One possible explanation is that planetary perturbations on stream meteoroids are significant over long time scales, even for high-inclination streams such as the Perseids, while the Harris model ignored planetary perturbations.

Little structure is evident in the mean ZHR profile with the possible exception of a maximum near λ=140.9° and a slight maximum at λ=139.5°. The latter is undoubtedly related to the fact that the outburst component of the stream has not been entirely filtered from these data. In addition to these local features, a broad plateau is clearly visible in the flux profile immediately following the main maximum, a consequence of the increase in *r* after the main maximum.

The lack of strong sub-maxima is an expected result, as the smoothing procedures and addition of all data act as a filter to suppress any short period features from the mean profile, with sub-maxima being visible primarily in the yearly profiles. Stable sub-maxima in long-term Perseid data have been noted previously, particularly in radar data. Table 3.3 summarizes the reported locations of past sub-maxima detailed in the literature as well as the location of the main maximum. Previous visual and radar studies have suggested recurrent sub-maxima near λ=140.5°, but this is not supported by our mean profile. There are indications of a sub-maximum near this position in the 1993 and 1994 profiles; it is worth noting that these years had far better coverage after the main maximum than any of the other years. The most convincing candidates, however, for true sub-maxima in these years are located in the region λ=140.2°-140.3°. That sub-maxima are present in some years appears probable given the high statistical weight of the visual

reports in the present study, but the stability of such structures over many years is still questionable based on our results. Such structures may be linked with mean motion resonances operating in the Perseid stream as has been suggested by Wu and Williams (1995). Local maxima may simply be manifestations of groups of meteoroids with a common ejection origin sharing similar values of nodal longitude and semi-major axes and thus being more numerous in one year than in others. This sharp variation in the flux would be a direct result of a sharp peak in the distribution of semi-major axis within such a meteoroid sub-population.

In contrast, the main maximum shows a generally stable peak flux. Indeed, the peak flux from 1988-1994 associated with the main maximum varies from the average value $\Phi_{6.5\ peak}= (2.5\pm0.4)\times10^{-2}$ meteoroids km^{-2} $hour^{-1}$ for Perseids with $M_v>+6.5$ by less than 30%. This result contradicts past visual results, which suggest large variations in the flux. Zvolankova (1984) and Lindblad (1986) report variations of more than a factor of two in peak rates from visual observations made between the years 1944-1953 and 1953-1981 respectively. We suggest that these apparent variations are the result of biased sampling in past visual observations due to uneven observer coverage.

The changes in flux associated with the main maximum are given in Table 3.2 The average value for $\Phi_{6.5\ peak}$ of $(2.5\pm0.4)\times10^{-2}$ and of $(2.9\pm0.4)\times10^{-3}$ for $\Phi_{3.5\ peak}$, are in close agreement with the results of Kaiser et al. (1966) and Andreev et al. (1987) who derive an average $\Phi_{6.5\ peak}=(3.4\pm0.5)\times10^{-2}$ and $\Phi_{3.5\ peak}=3.7\times10^{-3}$, respectively from radar observations.

Table 3.3: Locations of the main maximum and literature reports of sub-maxima from recent radar and visual observations of the Perseids. λ is the reported position of the main maximum and λ_{sub} is the position of additional sub-maxima detected in the given year(s). Possible locations of sub-maxima from this analysis are also shown; values in parentheses are less certain.

Year(s)	λ	λ_{sub}	Source
1980	139.92±0.04°	-	Mason and Sharp (1981)
1958-1962, 1972	139.89±0.04°	139°;139.5°	Simek (1987)
1980-1985		140.5°;142°	
1958-1964	139.91±0.03°	140.5°	Simek and McIntosh (1986)
1953-1978	139.9±0.04°	140.46°	Lindblad and Simek (1986)
1953-1981	140.11°	140.45°	Lindblad (1986)
1964-1981	139.7±0.2°	-	Andreev et al. (1987)
1989	139.8±0.09°	140.1°;140.3°	This work
		(140.9°)	
1991	139.94±0.04°	(140.34°); 140.9°	This work
1993	139.91±0.04°	140.2°; (140.5°)	This work
1994	139.84±0.04°	140.3°; (140.5°)	This work

Table 3.4: The population index, *r*, and the quantity of data that each *r* value is derived from for the average profile from 1988-1994.

λ	*r*	No. of Observers	No. of Perseids
139.045°	1.930±0.018	172	11,931
139.354°	1.886±0.022	101	10,257
139.362°	1.913±0.021	118	11,369
139.508°	2.054±0.032	43	2,806
139.562°	2.049±0.039	27	1,870
139.752°	1.900±0.068	13	1,140
139.828°	1.992±0.032	70	9,001
139.878°	2.099±0.027	83	11,641
140.011°	2.055±0.034	61	5,664
140.107°	1.873±0.031	76	5,389
140.224°	1.987±0.024	117	9.660
140.307°	2.022±0.022	162	15,257

140.370°	2.049±0.029	96	9,638

The variation in the population indexes of the stream shows several features (see Figs. 3.10b and 3.11b). The most obvious is the asymmetry in particle makeup in the day leading to the main maximum, when *r* is consistently low, compared to after the main maximum, when *r* shows a significant increase. The average value of *r* for the remainder of the profile, both before and after the maxima, is remarkably constant near 2.15. Two pronounced maxima in *r* are also evident near the time of the activity maxima. The first maxima in *r* occurs at $\lambda=139.55°\pm 0.07°$ and the second at $\lambda=139°88\pm0.06°$. That these features are statistically significant can be assessed from Table 3.4 where the amount of magnitude data used to derive each *r* value is given. These locations are potentially linked to the different evolutionary components of the stream. The first is probably related to the outburst component, which is still present despite our attempt to remove the central portions of the outburst activity in each year. The young meteoroidal material associated with the latest return of Swift-Tuttle is rich in smaller meteoroids as would be expected for recent ejecta. The main maximum is also rich in fainter meteors, indicating the presence of comparatively young material.

A single local minimum in the population of small meteoroids just before maximum has been previously noted by Mason and Sharp (1981). Andreev et al. (1987) found a local maximum in the proportion of small meteoroids at the time of maximum from radar data. It seems probable that the different ages of the outburst and core components of the stream are manifest not only in higher flux but also in differences in the average meteoroid population relative to the background population, and that recent ejections of fresher meteoroids have significantly different *r* values as shown by these visual data.

The outburst component of the stream has only been recognized in visual observations over the last few years (cf. Roggemans, 1989), though Lindblad and Porubcan (1994) have shown that photographic records of Perseid activity dating back to the 1950's had an earlier peak near the present nodal longitude for 109P/Swift-Tuttle. Simek and Pecina (1996) also detected the presence of the outburst peak as early as 1986 in the Ondrejov radar data and suggest that the sub-maxima reported at $\lambda=139.5°$ by

Simek (1987) in earlier radar data may also be a detection of the outburst component of the stream. This component has been widely associated with the return of 109P/Swift-Tuttle to perihelion in 1992 and is generally associated with material from the last perihelion passage of Swift-Tuttle in 1862 (Wu and Williams 1993; Williams and Wu 1994; Jones and Brown 1996).

The position of the maximum of the outburst component of the stream given in Table 3.2 shows no clear variation as a function of the year. The relative magnitudes of the peaks are shown in Fig. 3.12a where the flux at the outburst peaks are given relative to $\Phi_{6.5\ peak}$. Here a clear demarcation occurs, with activity being weak before 1991 and strong thereafter. This sudden change in the outburst component, rather than a gradual increase in flux as predicted by model calculations assuming all new activity to result from 1862 ejecta (Williams and Wu 1994), suggests that meteoroids encountered before 1991 may have a different origin. On the basis of model calculations, Jones and Brown (1996) ascribe the material from 1988-1990 as being almost exclusively from the 1737 and 1610 passages of Swift-Tuttle, with meteoroids from the 1862 passage first encountered in significant quantities in 1991 (see Chapter 4).

The locations of the visual maxima in these years are very similar to those reported from overdense radar observations. Watanabe et al. (1992) analyzed the 1991 Perseid return with the Kyoto MU-radar and determined the time of peak for the outburst component to be λ=139.6, in good agreement with our results. They also found that the outburst peak flux was 3.4±0.8 times that of the main maximum.

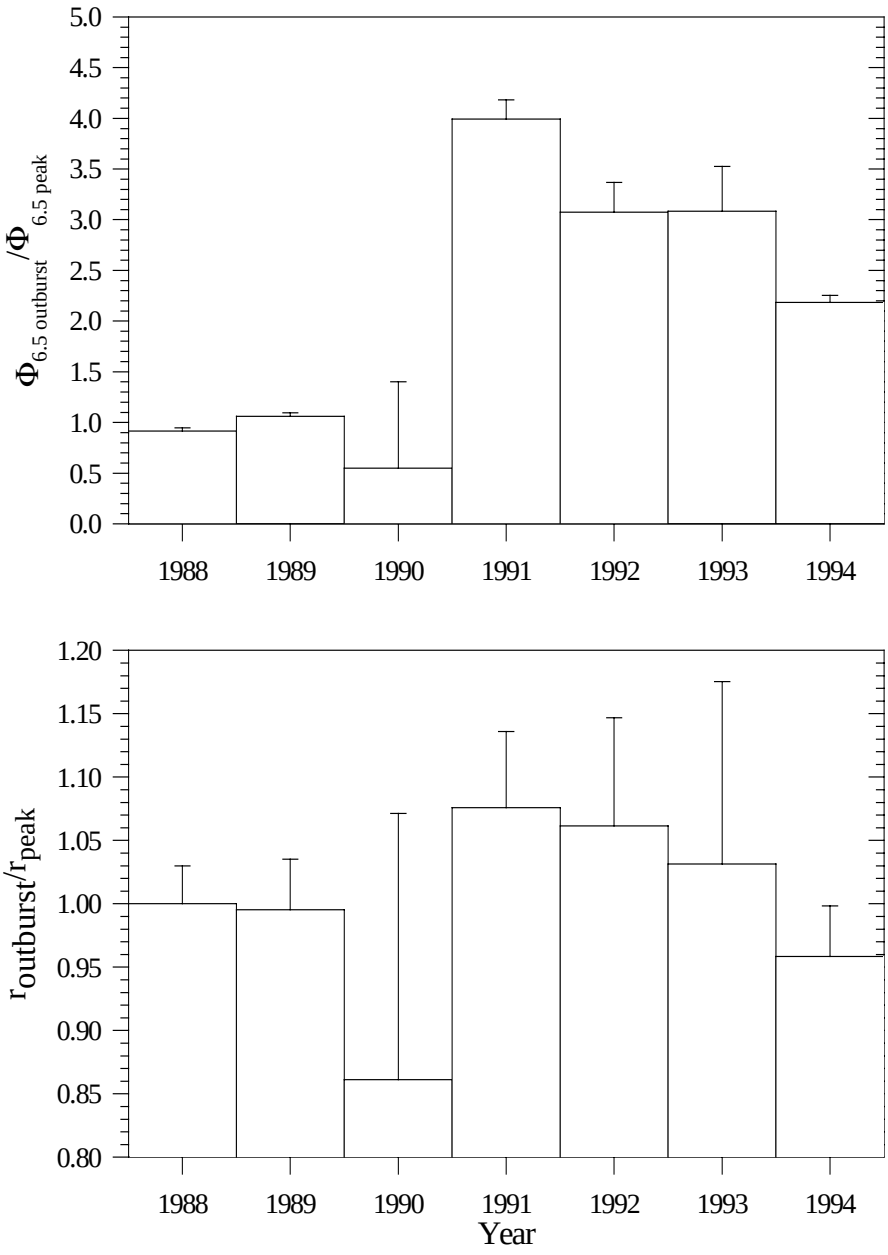

Fig 3.12: The relative magnitude of the peak flux (a - top) of the outburst component of the Perseid stream from 1988-1994 relative to the flux of the normal maximum. b - bottom, the change in the particle composition during the outbursts from 1988-1994 relative to the particle distribution at the time of the normal peak.

This result applies to meteors in the magnitude range $0>M_v>+3$ and is similar to the ratio of peak fluxes we find between the outburst peak and the core maximum in 1991 of 3.2 over the same magnitude range. For comparison, Simek and Pecina (1996) used the Ondrejov radar data and found the maximum to be located at an average position of $\lambda=139.58°\pm0.04°$ in the interval 1986-1994.

The particle composition of the outburst component of the stream relative to the main peak is shown in Fig.3.12b, where the ratio of the respective population indices has been plotted. Watanabe et al. (1992) report an increase in the proportion of large meteoroids during the outburst in 1991 and this notion has been variously supported by qualitative reports from observers during other Perseid outbursts (cf. Pin-xin, 1992). There is little question that the number of bright Perseids increases during the outbursts. Fig 3.12b, however, shows that the proportion of bright meteors during the outbursts does not differ substantially from the main peak. Thus the mass distribution of the outburst in all years, as measured by *r*, does not differ, within error, from the population associated with the core component of the stream. This contradicts the conclusions of Watanabe et al. (1992) and is consistent with the earlier observation of a maximum in the *r* values near the time of both maxima.

3.6 Summary and Conclusions

From the flux data and particle population presented here, it is evident that several outstanding features of the Perseid stream need to be addressed when attempting to model it. These include:

- The asymmetry in the background Perseids and the symmetry in the core population as defined by the locations of the 1/4-width (2.58°±0.07° before the main maximum and 2.35°±0.07° after maximum) and the 1/2-width (1.06°±0.07° before maximum and 1.04°±0.07° after maximum) positions.

- The location and magnitude of the outburst maxima for each year given in Table 3.2.

- The location and magnitude of the mean activity maximum associated with the core population at λ=139.96°±0.05° and with $\Phi_{6.5\ peak}=(2.5\pm0.4)\times10^{-2}$ meteoroids km^{-2} hour^{-1}.

- The change in particle composition across the stream, particularly in the region near the maxima in *r* at λ=139.55°±0.07° and at λ=139.88°±0.06°.

- The apparent similarity between the meteoroid populations associated with the outburst and core population.

- The broad shoulder in flux after the core maximum.

- The differing slopes in the branches of the outburst profile and the asymmetry in these profiles.

- The origins of the background, outburst and core populations.

Other characteristics not clearly discernable in these data, such as the possible presence of a sub-maximum near λ=140.2°-140.3° or at λ=140.5° and the existence of ephemeral sub-maxima at various locations after the core maximum in different years, need further observational confirmation.

Similarly, the location and the size of the mean radiant for the shower and its likely variation during the course of activity of the shower are important diagnostics for use in modelling.

From these data it is apparent that the Perseid meteoroid stream is highly dynamic and rich in structure. The complexities of the Perseids can only be understood in the context of a complete numerical model of the stream, which can explain features detected through observations, such as those described here.

References

Ahnert-Rohlfs, E. 1952. On the structure and the origin of the Perseid meteoroid stream. *Veröffentlichungen der Sternwarte Sonneberg* **2**, 5-38.

Andreev, G. V., L. N. Rubtsov, and N. V. Tarasova. 1987. On the spatial structure of the Perseids meteor stream. In *First GLOBMET Symposium* (R. G. Roper, Ed.), p. 39. ICSU-SCOSTEP, Urbana, Illinois.

P. Brown and J. Rendtel (1996) The Perseid Meteoroid Stream: Characterization of Recent Activity from Visual Observations, *Icarus*, **124**, 414-428.

Harris, N. W., K. C. C. Yau, and D. W. Hughes. 1995. The true extent of the nodal distribution of the Perseid meteoroid stream. *Mon. Not. R. Astron. Soc*. **273**, 999-1015.

Hasegawa, I. 1993. Historical records of meteor showers. In *Meteoroids and Their Parent Bodies* (J. Štohl and I. P. Williams, Eds.), p. 209. Astronomical Inst., Slovak Acad. Sci., Bratislava.

Jones, J. and P. Brown. 1993. Sporadic meteor radiant distributions: orbital survey results. *Mon. Not. R. Astron. Soc*. **265**, 524-532.

Jones, J. and P. Brown. 1996. Modelling the orbital evolution of the Perseid meteoroids. In *Physics, Chemistry and Dynamics of Interplanetary Dust* (B. Å. S. Gustafson and M. S. Hanner, Eds.), p. 105. Astronomical Society of the Pacific.

Kaiser, T. R., L. M. G. Poole, and A. R. Webster. 1966. Radio-echo observations of the major night-time streams. I. Perseids. *Mon. Not. R. Astron. Soc*. **132**, 224-237.

Koschack, R., R. Arlt and J. Rendtel. 1993. Global analysis of the 1991 and 1992 Perseids. *WGN J. IMO* **21(4)**, 152-168.

Koschack, R. 1995. Analyses and Calculations. In *Handbook for Visual Meteor Observers* (J. Rendtel, R. Arlt and A. McBeath, Eds.), pp. 280-289. IMO, Potsdam.

Koschack, R., and R. L. Hawkes. 1995. Observing instructions for major meteor showers. In *Handbook for Visual Meteor Observers* (J. Rendtel, R. Arlt and A. McBeath, Eds.), pp. 42-74. IMO, Potsdam.

Koschack, R., and J. Rendtel. 1988. Number density in meteor streams. *WGN J. IMO* **16**, 149-157.

Koschack, R., and Rendtel, J. 1990a. Determination of spatial number density and mass index from visual meteor observations. *WGN J. IMO* **18**, 44-59.

Koschack, R., and J. Rendtel, J. 1990b. Determination of spatial number density and mass index from visual meteor observations (II). *WGN J. IMO* **18**, 119-141.

Koschack, R., and P. Roggemans. 1991. The 1989 Perseid meteor stream. *WGN J. IMO* **19**, 87-99.

Kresáková, M. 1966. The magnitude distribution of meteors in meteor streams. *Contr. Skalnaté. Pleso* **3**, 75-109.

Kronk, G. W. 1988. *Meteor Showers: A Descriptive Catalog*. Enslow, New Jersey.

Lindblad, B. A. 1986. Structure and activity of the Perseid meteor stream from visual observations 1953-1981. In *Asteroids, Comets, Meteors II* (C.-I. Lagerkvist, B. A. Lindblad, H. Lundstedt, and H. Rickman, Eds.), p.531. Reprocentralen, Uppsala.

Lindblad, B.A. and V. Porubcan 1994. The activity and orbit of the Perseid meteor stream. *Planet. Sp. Sci.* **42**, 117-123.

Lindblad, B. A. and M. Šimek. 1986. The activity curve of the Perseid meteor stream from Onsala radar observations 1953-78. In *Asteroids, Comets, Meteors II* (C.-I. Lagerkvist, B. A. Lindblad, H. Lundstedt, and H. Rickman, Eds.), p.537. Reprocentralen, Uppsala.

Lovell, A.C.B. 1954. *Meteor Astronomy*. Pergamon, London.

Marsden, B. G. 1973. The next return of the comet of the Perseid meteors. *Astron. J.* **78**, 654-662.

Mason, J. W., and I. Sharp. 1981. The Perseid meteor stream in 1980. *JBAA* **91**, 368-390.

McKinley, D. W. R. 1961. *Meteor Science and Engineering*. McGraw-Hill, Toronto.

Olson, D. W., and R. L. Doescher. 1993. Meteor observations on August 10-11, 1863. *WGN J. IMO* **21**, 175-181.

Pin-Xin, X. 1992. The 1992 Perseid outburst in China. *WGN J. IMO* **20**, 198.

Rendtel, J., P. Brown, and S. Molau. 1996. The 1995 outburst and possible origin of the α- Monocerotid meteoroid stream. *Mon. Not. R. Astron. Soc*. **279**, L31-L36.

Roggemans, P. 1989. The Perseid Meteor Stream in 1988: A Double Maximum! *WGN J. IMO* **17**, 127-137.

Schiaparelli, G. V. 1867. Sur les Étoiles Filantes, et spécialement sur l'identification der Orbites des Essaims d'Août et de Novembre avec celles des Comètes de 1862 et de 1866. *Comptes Rendus* **64**, 598-599.

Šimek, M. 1987. Perseid meteor stream mean profile from radar observations in Czecheslovakia. *BAC* **38**, 1-6.

Šimek, M., and B. A. McIntosh. 1986. Perseid meteor stream: mean flux curve from radar observations. *BAC* **37**, 146-155.

Šimek, M., and P. Pecina. 1996. Activity of the new filament of the Perseid meteor stream. In *Physics, Chemistry and Dynamics of Interplanetary Dust* (B. Å. S. Gustafson and M. S.Hanner, Eds.), p. 109. Astronomical Society of the Pacific.

Verniani, F. 1973. An analysis of the physical parameters of 5759 faint radio meteors. *J. Geophys. Res*. **78**, 8429-8462.

Watanabe, J-I., T. Nakamura, M. Tsutsumi, and T. Tsuda. 1992. Radar Observations of the strong activity of a Perseid meteor shower in 1991. *PASJ* **44**, 677-685.

Williams, I. P., and Z. Wu. 1994. The current Perseid meteor shower. *Mon. Not. R. Astron. Soc.* **269**, 524-528.

Wu, Z., and I. P. Williams. 1993. The Perseid meteor shower at the current time. *Mon. Not. R. Astron. Soc*. **264**, 980-990.

Wu, Z., and I. P. Williams. 1995. Gaps in the semimajor axes of the Perseid meteors. *Mon. Not. R. Astron. Soc*. **276**, 1017-1023.

Yau, K., D. Yeomans, and P. Weissman. 1994. The past and future motion of comet P/Swift-Tuttle. *Mon. Not. R. Astron. Soc*. **266**, 303-316.

Zvolánková, V. 1984. Changes in the activity of the Perseid meteor shower 1944-1953. *Contr. Obs. Skalnaté Pleso* **12**, 45-75.